Research Paper

ISSN 1225-6153
Online ISSN 2287-8955

Microstructure and Mechanical Property in the Weld Heat-affected Zone of V-added Austenitic Fe-Mn-Al-C Low Density Steels

Joonoh Moon*,† and Seong-Jun Park*

*Ferrous Alloy Department, Advanced Metallic Materials Division, Korea Institute of Materials Science, Changwon 642-831, Korea

†Corresponding author : mjo99@kims.re.kr

(Received August 3, 2015 ; Revised September 30, 2015 ; Accepted October 1, 2015)

Abstract

Microstructure and tensile property in the weld heat-affected zone (HAZ) of austenitic Fe-Mn-Al-C low density steels were investigated through transmission electron microscopy analysis and tensile tests. The HAZ samples were prepared using Gleeble simulation with high heat input welding condition of 300 kJ/cm, and the HAZ peak temperature of 1200℃ was determined from differential scanning calorimetry (DSC) test. The strain- stress responses of base steels showed that the addition of V improved the tensile and yield strength by grain refinement and precipitation strengthening. Tensile strength and elongation decreased in the weld HAZ as compared to the base steel, due to grain growth, while V-added steel had a higher HAZ strength as compared than V-free steel.

Key Words : Low density steel, Heat-Affected Zone (HAZ), Grain refinement, Precipitation strengthening Vanadium carbide

1. Introduction

In recent years, many researches have focused on the development of low density steels for automotive industry, in energy saving concern.[1)] In the literatures, Fe-Mn-Al-C steels have received much attention as a candidate material for low density automotive steel for past several decades.[1-6)] Frommeyer and Brüx[2)] reported high-strength low density steels, the so-called TRIPLEX steels. TRIPLEX steel consisted of three main phases of austenite matrix, 5-15 vol.% ferrite and nano-size κ-carbide below 10 vol.%. Recently, Kim et al.[3)] developed high performance low density steel, which had higher specific strength than Ti alloys. Interestingly, the developed steel showed high ductility despite the precipitation of brittle FeAl type intermetallic compound (B2). Yoo and Park[4)] investigated the tensile deformation behavior of a Fe-27.8Mn-9.1Al-0.79C steel and reported that continuous strain hardening behavior occurred by microband-induced plasticity (MBIP). Lee et al.[5)] and Park et al.[6)] explored the tensile deformation behavior of duplex grade Fe-Mn-Al-C low density steel using a nanoindentation and in situ electron backscattered diffraction (EBSD).

Most previous investigations actively used fine κ-carbide as a strengthener of Fe-Mn-Al-C steels[1-2)], while few studies have tried to use microalloying elements, such as Nb and V.[7)] Their results clearly showed that Nb and/or V addition had an effect on the grain refinement, but didn't show detailed microscopic analysis. In addition, it is somewhat surprising that the study on the weld characteristics of Fe-Mn-Al-C steels is not available in the literature.

With all this in mind, in this paper we developed austenitic Fe-30Mn-9Al-0.9C low density steel containing V and investigated its microstructure and tensile property in the base metal and the HAZ. The simulated HAZ samples were prepared by Gleeble simulator with high heat input welding condition of 300 kJ/cm. The microstructures were analyzed using scanning electron microscopy (SEM), and transmission electron microscopy (TEM). In addition, we evaluated the mechanical property using tensile tests, and discussed about correlation between microstructure and tensile property.

2. Experimental procedures

The chemical composition of tested steels in this study is given in Table 1. Ingots for two Fe-Mn-Al-C steels were

Table 1. Chemical composition of tested alloys, and grain size of base steel

Alloys	Chemical composition, in wt%					Grain size of base steel, μm
	C	Mn	Al	V	Fe	
A steel	0.80	31.5	8.7	-	Bal.	80.2
B steel	0.86	31.6	8.6	0.50	Bal.	16.8

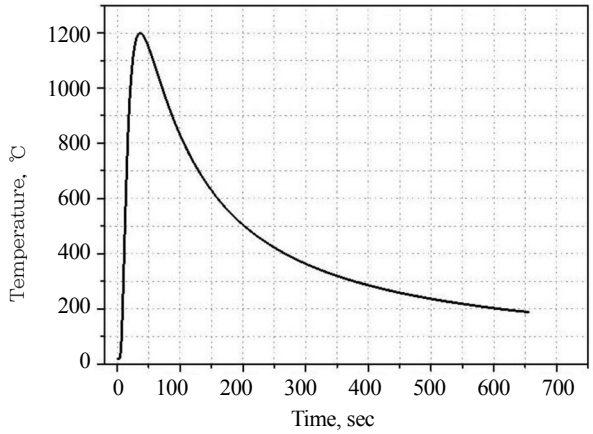

Fig. 1 Thermal cycle of the HAZ simulated by Gleeble simulator

fabricated using a commercial vacuum-induction melting (VIM) furnace. Compared to steel A, steel B additionally contained microalloying elements of V which can form carbide. Ingots were homogenized for 2 h at 1150℃ and then hot-rolled into plate. The base steels were prepared after solution-treatment for 2 h at 1050℃ and water quenching. The HAZ samples were prepared using Gleeble simulation (Gleeble-1500, DSI, USA). A schematic illustration of the thermal cycle is shown in Fig. 1. This thermal cycle was calculated using Rosenthal's heat-flow equation.[8-9] The HAZ thermal cycle in Fig. 1 was calculated for a heat input of 300 kJ/cm and a peak temperature of 1200℃. Here, the HAZ peak temperature was determined from differential scanning calorimetry (DSC) test. Fig. 2 shows the DSC test result of steel A and indicates that the phase transitions including melting occurred at over 1,333℃, i.e., the austenite phase is stable up to 1,333℃ and thus we selected 1,200℃ as a HAZ peak temperature. Tensile stress-strain relation of base steels and HAZ samples (ASTM E8M) was obtained through a tensile test machine (INSTRON 5882, Canton, MA, USA) at a nominal strain rate of 1.33×10^{-3} s^{-1}. The austenite grain size of base steels was measured by the linear intercept method according to ASTM standard. The microstructures were observed using a SEM (JSM-7001F, JEOL, Japan) after mechanical polishing and chemical etching in a mixed solution of 90 ml ethanol and 10 ml nitric acid. VC particles were observed by TEM (JEM-2100F, JEOL, Japan), and identified by a selected area diffraction pattern (SADP) analysis. Thin foil specimen for TEM analysis

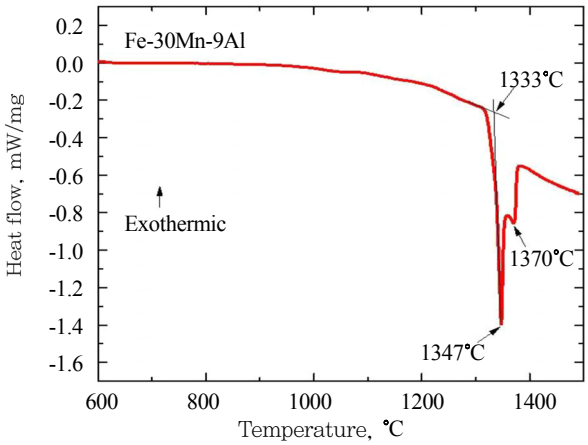

Fig. 2 DSC data during heating of steel A

were prepared by twin-jet electrolytic polishing at 20 V and 200 mA with a mixed solution of 10 % perchloric acid and 90 % methanol at -30℃.

3. Results and discussion

3.1. Microstructure and tensile properties of the base steels

Fig. 3 shows SEM micrographs of the base metal after solution treatment. The matrix consisted of austenite containing some annealing twins. Compared to steel A, lots of particles were observed in the matrix of steel B, and they were randomly distributed regardless of the grain boundaries or grain interior. Fig. 4 shows the results of TEM analysis. Steel A consisted of full austenite matrix shown in Fig. 4(a), while steel B contained fine carbides within the austenite matrix as shown in Fig. 4(b) and here these particles were identified as VC particle of MX-type carbides through SAD pattern analysis. The SAD patterns in Fig. 4(c) and (d) show that the VC exhibits the cube-cube orientation relationship $[011]_\gamma$ // $[011]_{VC}$ with respect to the austenite matrix.[10] Compared to steel A, steel B contained V, which is strong carbide former. Kalashnikov et al.[7] investigated the particles in low density steel having similar chemical composition with the steel tested in this study.

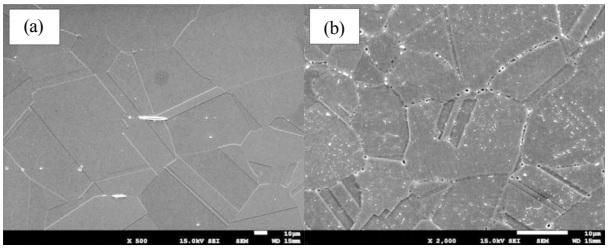

(a) steel A (b) steel B

Fig. 3 SEM micrographs of the base steels

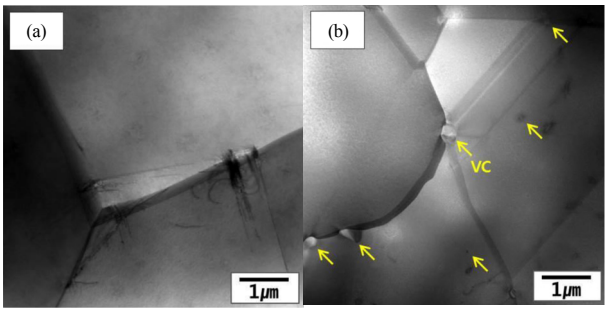

(a) bright field image of steel A (b) bright field image of steel B

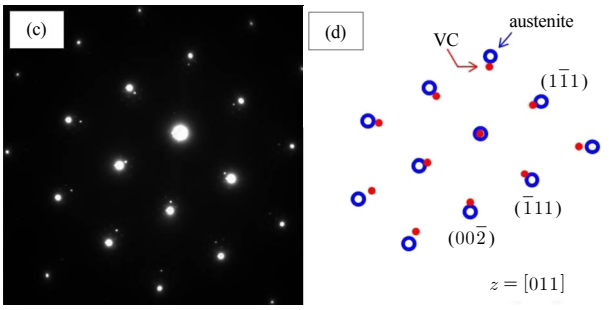

(c) SAD pattern with Z=[011] (d) computer simulated SAD pattern

Fig. 4 TEM micrographs of base steels

With considering the report presented in the literature[7], it is conceivable that VC particles in Fig. 4(b) were nucleated during solidification in VIM process, and they were coarsen during solution treatment at 1250℃. Mean- while, Fig. 3 shows that the austenite grain size of steel B was much smaller than that of steel A and then the measured results are listed in Table 1. This might be due to the effect of grain growth inhibition by VC particles, during solution treatment.

Fig. 5 shows the tensile strain-stress curves of base steels, and indicates that steel B had higher yield and tensile strength. This might be due to the effect of grain refinement and precipitation strengthening. The Orowan mechanism is well-known as the main precipitation streng-thening mechanism.[11-12] Generally, the strength increase by Orowan mechanism is expressed as

$$\tau_{O_{ro}} = \frac{G \cdot b}{\lambda} \quad (1)$$

where G is shear modulus of matrix and b is Burgers vector. The parameter λ is the interparticle spacing between particles which is given as

$$\lambda = \frac{4 \cdot (1-f) \cdot r}{3f} \quad (2)$$

where f is the particle volume fraction and r is the particle radius. Eqs. (1) and (2) indicate that the precipitation hardening by the Orowan mechanism depends on the size and

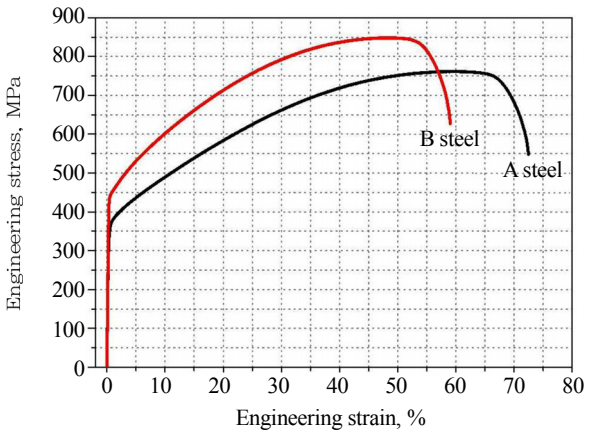

Fig. 5 Tensile test results of the base steels

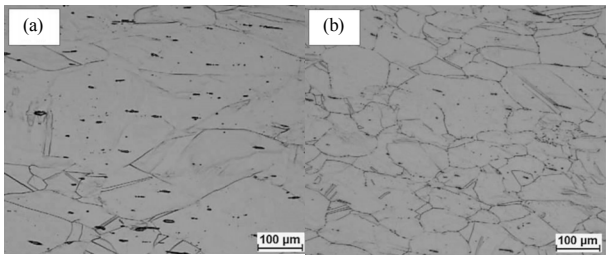

(a) steel A (b) steel B

Fig. 6 Optical micrographs of the HAZs

fraction of particles, i.e., fine particles with high fraction are the most effective for precipitation hardening. As shown in Fig. 3 and Table 2, steel B contained fine VC particles with high fraction and thus steel B had higher strength of more than 100MPa as compared to steel A. Meanwhile, the elongation decreased with increase in strength.

3.2. Microstructure and tensile properties of the HAZ samples

Fig. 6 shows the optical micrographs of the simulated HAZ samples. The HAZ samples consisted of austenite and then their grain sizes increased as compared to the base steel shown in Fig. 3. This might be due to grain growth during high temperature thermal cycle in the HAZ. Never theless, the grain size of steel B was smaller than that of steel A and this is because stable VC in steel B contributed to the grain growth inhibition in the HAZ. Mean- while, note that some of black spots in Fig. 6(a) were MnS inclusions and the others were pits caused by over-etching. Fig. 7 shows the tensile strain-stress curves of HAZs, and indicated that steel B had still had higher yield and tensile strength in the HAZ as compared to steel A. This might be also due to the effect of grain refinement and precipitation strengthening. Meanwhile, tensile strength and elongation decreased in the weld HAZ as compared to the base steel, which may be due to grain growth as mentioned above. It

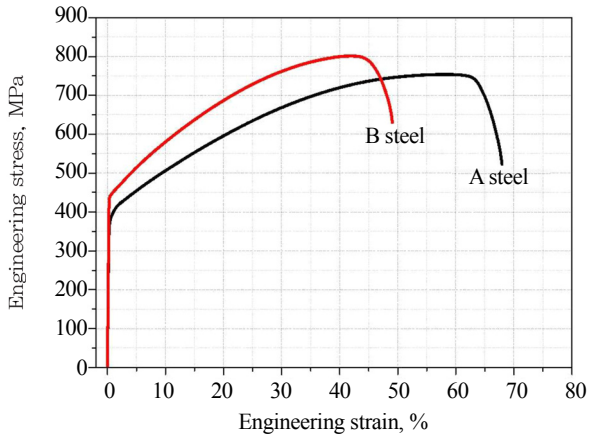

Fig. 7 Tensile test results of the HAZs

is somewhat interesting that yield strength in Table 2 strength increased rather than deterioration in the HAZ as compared to base steel despite grain growth. In the future, we will investigate the reason of yield strength increase in the HAZ with careful microstructure analysis.

4. Concluding remarks

Effect of V addition on the microstructure and tensile properties in the base steel and the HAZ of austenitic Fe-30Mn-9Al-0.9C low density steels were explored. The addition of V led to the improvement of tensile properties by the grain refinement and precipitation hardening, resulting from the precipitation of VC particles. VC particles exhibited the cube-cube $[011]_{\gamma}$ // $[011]_{VC}$ orientation relationship with the austenite matrix. Tensile strength and elongation decreased in the weld HAZ as compared to the base steel, which may be due to grain growth during high temperature thermal cycle in the HAZ, while V-added steel had a higher HAZ strength than V-free steel.

Acknowledgements

This work was supported by the Materials and Components Technology Development Program (10048157) funded by the Ministry of Trade, Industry and Energy (MOTIE, South of Korea).

References

1. Kim H, Suh DW, Kim NJ, Fe-Al-Mn-C lightweight structural alloys: a review on the microstructures and mechanical properties. *Sci. Technol. Adv. Mater*. 14 (2013), 1-11
2. Frommeyer G, Brüx U, Microstructures and mechanical properties of high-strength Fe-Mn-Al-C light-weight TRIPLEX steels. *Steel Res. Int*. 77 (2006), 627-633
3. Kim SH, Kim H, Kim NJ, Brittle intermetallic compound makes ultrastrong low-density steel with large ductility. *Nature* 518 (2015), 77-79
4. Yoo JD, Park KT, Microband-induced plasticity in a high Mn-Al-C light steel. *Mater. Sci. & Eng. A* 496 (2008), 417-424
5. Lee K, Park SJ, Choi YS, Kim SJ, Lee TH, Oh KH, Han HN, Dual-scale correlation of mechanical behavior in duplex low-density steel. *Scripta Mater*. 69 (2013), 618-621
6. Park SJ, Hwang B, Lee KH, Lee TH, Suh DW, Han HN, Microstructure and tensile behavior of duplex low-density steel containing 5 mass% aluminum. *Scripta Mater*. 68 (2013), 365-639
7. Kalashnikov IS, Ermakov BS, Aksel'rad O, Pereira LK, Alloying of steels of the Fe-Mn-Al-C system with refractory elements. *Metal Sci. & Heat Treatment* 43 (2001), 493-436
8. Easterling K, Introduction to the physical metallurgy of welding (1st Edition), 1983; 33-35
9. Moon J, Lee C, Precipitation and Precipitate Coarsening Behavior According to Nb Addition in the Weld HAZ of a Ti-containing Steel. *Journal of KWJS*, 26 (1) (2008), 76-82 (in Korean)
10. Furuhara T, Shinyoshi T, Miyamoto G, Yamaguchi J, Sugita N, Kimura N, Takemura N, Maki T, Multiphase crystallography in the nucleation of intergranular ferrite on MnS+V(C, N) complex precipitate in austenite. *ISIJ Int.* 43 (2003), 2028-2037
11. Moon J, Kim S, Jang J.-I, Lee J, Lee C, Orowan strengthening effect on the nanohardness of the ferrite matrix in microalloyed steels. *Mater. Sci. & Eng*. A, 487 (2008), 552-557
12. Moon J, Lee C, Microstructure Evolution and Its Effect on Strength during Thermo-mechanical Cycling in the Weld Coarse-grained Heat-affected Zone of Ti-Nb Added HSLA Steel. *Journal of KWJS*, 31 (6) (2013), 44-49 (in Korean)